

Polarized-neutron study of the magnetic moment distribution in *PdMn* alloys*

J. W. Cable and L. David†

Solid State Division, Oak Ridge National Laboratory, Oak Ridge, Tennessee 37830

(Received 21 March 1977)

Polarized-neutron diffuse-scattering methods were used to determine the spatial distribution of the magnetic moments in *PdMn* alloys containing 0.23-, 0.46-, 0.99-, and 1.91-at.% Mn. The measurements, made on polycrystalline samples at 4.2 K in an applied field of 45 kOe, show a moment of about $4\mu_B$ localized at the Mn sites. The lower-concentration cross sections tend to increase at small reciprocal-lattice vector \vec{K} , as expected for such "giant-moment" systems, while the two higher-concentration alloys show an anticorrelation corresponding to Mn spin reversal and/or positional short-range order. The cross sections are analyzed by assuming that the magnetic moment on a Pd atom depends on both its magnetic and chemical environment.

INTRODUCTION

Recent magnetization measurements^{1,2} on dilute *PdMn* alloys show giant-moment behavior similar to that observed earlier for the³ *PdFe* and⁴ *PdCo* systems. At low concentrations of Fe or Co impurities in Pd the magnetic moment per impurity is about $10\mu_B$, but neutron diffuse scattering⁵⁻⁸ shows only about $3\mu_B/\text{Fe}$ and $2\mu_B/\text{Co}$ localized at the impurity sites, with the remainder being induced in the surrounding Pd atoms. For Mn impurities the giant moment is about $7.5\mu_B$ per impurity^{1,2} but there is some uncertainty regarding what part of that is localized at Mn sites. Specific-heat data⁹ yield a spin value of 2.4 ± 0.2 which suggests $5\mu_B$ at the Mn sites and this is supported by neutron diffuse-scattering results¹⁰ which give $(5.5 \pm 0.5)\mu_B$ at the Mn site. However, this implies an electronic configuration with only five *d* electrons for Mn dissolved in a transition metal whereas at least six *d* electrons and a maximum moment of $4\mu_B/\text{Mn}$ are expected. Also, this $5.5\mu_B$ value is larger than was obtained by paramagnetic scattering from a 10-at.% Mn alloy $[(3.3 \pm 0.4)\mu_B]$ ¹¹ and by Bragg scattering from an ordered 25-at.% Mn alloy $[(4.0 \pm 0.2)\mu_B]$.¹² The diffuse scattering measurement¹⁰ was made with unpolarized neutrons at a sample temperature near the Curie temperature and since this method measures all moment-moment spatial correlations, high-moment values could be obtained in the critical region. We decided that a determination of the Mn moment in Pd by the polarized-neutron diffuse-scattering method was desirable. Here, only magnetic moment-site occupation correlations appear and the measurements are not complicated by possible critical scattering effects.

EXPERIMENT

In the polarized-neutron diffuse-scattering experiment, the sample is magnetized perpendicular

to the scattering plane. In this geometry, the difference between the cross sections for incident neutrons polarized parallel and antiparallel to the magnetization is

$$\Delta \frac{d\sigma}{d\Omega}(\vec{K}) = 1.08c(1-c)(b_i - b_h)\mathfrak{M}(\vec{K}), \quad (1)$$

where c is the impurity concentration, b_i and b_h are the impurity and host nuclear scattering amplitudes, and $c(1-c)\mathfrak{M}(\vec{K})$ is the Fourier transform of the moment-site occupation correlation, $\langle (p_{\vec{n}+\vec{R}} - c)\mu_{\vec{n}}(\vec{K}) \rangle$. Here, $p_{\vec{n}+\vec{R}}$ is the number of impurity atoms (0 or 1) at $\vec{n}+\vec{R}$ and $\mu_{\vec{n}}(\vec{K})$ is the moment-form factor product at site \vec{n} . For polycrystalline samples, the spherical average of $\mathfrak{M}(\vec{K})$ at large K approaches $\langle \mu_i(K) \rangle - \langle \mu_h(K) \rangle$ while, in the $K=0$ limit, $\mathfrak{M}(0) = S(0)$, $d\bar{\mu}/dc$ provided that the moment fluctuations are due to local environment effects. Here, $S(\vec{K})$ is the usual short-range order scattering function defined as the Fourier transform of $\langle (p_{\vec{n}+\vec{R}} - c)(p_{\vec{n}} - c) \rangle / c(1-c)$ and $d\bar{\mu}/dc$ is the concentration derivative of the average moment as determined from a bulk magnetization measurement.

Giant moments have been observed in the *PdMn* system up to 2.45-at.% Mn.² However, higher saturating fields are required with increasing Mn content because of Mn-Mn antiferromagnetic interactions. We have therefore confined our attention to dilute alloys containing nominally 0.25-, 0.50-, 1.00-, and 2.00-at.% Mn. The alloys were prepared from 99.91% Pd which was passed through an ion-exchange column to remove Fe and Co impurities. The resulting material contained 36-ppm Fe and 7-ppm Co with the major impurities being Au, Nb, and Pb (~200 ppm each). The powdered Pd was mixed with the appropriate amounts of powdered electrolytic Mn and the pressed powders were arc-melted and drop cast at 50-g ingots. These were machined into $0.7 \times 2 \times 2.8$ cm samples which were annealed at 1000 °C for 24 h. Chemical

analyses showed the actual compositions to be 0.23-, 0.46-, 0.99-, and 1.91-at.% Mn. Magnetization measurements were made on small pillar-shaped specimens cut from the neutron samples. Although limited to maximum fields of 10 kOe, magnetizations obtained at 4.2 K and 10 kOe were about 10% higher than those reported by Star, Foner, and McNiff,² thus confirming giant-moment behavior for these samples.

The neutron measurements were made with the samples at 4.2 K in an applied field of 45 kOe. Although the three lowest Mn content alloys have Curie temperatures below 4.2 K, the magnetization data² show 94%, 93%, 90%, and 85% of saturation is achieved for these four compositions at 4.2 K and 45 kOe. The diffuse intensity was measured inside of the first Bragg reflection with 1.07-Å neutrons. These were corrected for incident polarization and flipper efficiency and converted to absolute cross sections by calibration with a standard V scatterer. The $\mathfrak{M}(K)$ functions obtained from Eq. (1) with $b_{\text{Mn}} = -0.387$ and $b_{\text{Pd}} = 0.591 \times 10^{-12}$ cm are shown in Fig. 1. Here and through the remainder of this paper, spherical averages over K are denoted by dropping the vector notation on K . The average Pd moment is small ($<0.05\mu_B$) and $\mathfrak{M}(K)$ for $K > 1$ is essentially just $\langle \mu_{\text{Mn}} \rangle f_{\text{Mn}}(K)$. With $f_{\text{Mn}}(K) = \exp(-0.069K^2)$, which closely approximates the Mn^{+2} form factor in this K region, one obtains $\langle \mu_{\text{Mn}} \rangle = 3.6\mu_B$, $4.0\mu_B$, $3.5\mu_B$, and $3.5\mu_B$ at these

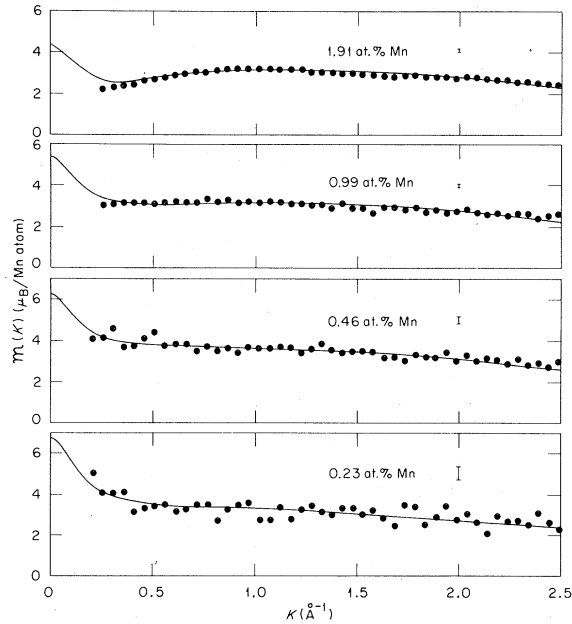


FIG. 1. $\mathfrak{M}(K)$ functions for some PdMn alloys at 4.2 K and 45 kOe. The solid curves are calculated from Eq. (6) using the moment values in Table I and $\Gamma = 0.975$. A small amount of positional short-range order is included (see text).

four compositions. At small K , $\mathfrak{M}(K)$ for the two more dilute alloys tends to increase, as would be expected if $\mathfrak{M}(0) = S(0)d\bar{\mu}/dc$. The two more concentrated alloys, however, show a decreasing $\mathfrak{M}(K)$ with decreasing K . This effect could arise either from positional short-range order or from antiferromagnetic alignment of Mn atom pairs, and is quite likely a combination of both effects. We show how these enter $\mathfrak{M}(K)$ in the following section.

MAGNETIC-ENVIRONMENT MODEL

Interatomic interactions are required to account for the long range of the moment disturbance produced in Pd by Mn, Fe, and Co.¹³ These can be treated within the molecular field framework by allowing the magnetic moment of an atom to depend on the magnetic environment of that atom. There may also be a short-range chemical environment effect on the moment which results from a disturbance of the electronic structure of the host due to the presence of the impurity. Both of these effects are included in a recently proposed¹⁴ magnetic environment model which successfully reproduces the $\mathfrak{M}(K)$ behavior of Ni-Cu,¹⁴ Ni-Rh,¹⁵ and dilute Ni-based alloys. We use this model to analyze the PdMn data.

It is assumed that the moment on a Pd atom at site \vec{n} depends on the molecular field $H_{\vec{n}}^*$ at that site and also on the number of impurity atom nearest neighbors $\nu_{\vec{n}}^*$. Thus,

$$\mu_{\vec{n}}^{\text{Pd}} = F(H_{\vec{n}}^*, \nu_{\vec{n}}^*), \quad (2)$$

with

$$\nu_{\vec{n}}^* = \sum_{\delta} p_{\vec{n}+\delta}^* \quad (3)$$

and

$$H_{\vec{n}}^* = \sum_{\delta} [J_{\text{PdPd}}(1 - p_{\vec{n}+\delta}^*)\mu_{\vec{n}+\delta}^* + J_{\text{PdMn}}p_{\vec{n}+\delta}^*\mu_{\vec{n}+\delta}^*], \quad (4)$$

where nearest-neighbor interactions are assumed and the sums are over the nearest neighbors. The Mn moment is assumed to have a fixed magnitude, but with possible spin reversal due to an antiferromagnetic Mn-Mn nearest-neighbor interaction. In this concentration range, the only Mn configurations occurring with significant probabilities are those with zero or one Mn nearest neighbors. If a Mn atom pair couples antiparallel and remains aligned with the Pd moments, then additional configurational assumptions are required to identify which of those Mn atoms has its spin reversed. We simplify this very complicated situation by assum-

ing that half of the Mn atoms with one Mn nearest neighbor undergo spin reversal. Thus, on the average, the Mn moment at site \vec{n} can be written

$$\mu_{\vec{n}}^{\text{Mn}} = \mu_{\text{Mn}}^0 \prod_6 (1 - p_{\vec{n}+\vec{\delta}}), \quad (5)$$

where μ_{Mn}^0 is the intrinsic Mn moment and the product is over nearest neighbors. With these moment assumptions, the K -dependent moment disturbance can be obtained in the manner outlined in Refs. 14 and 15. For a random alloy, one obtains

$$\begin{aligned} M(\vec{K}) = & \langle \mu_{\text{Mn}} \rangle f_{\text{Mn}}(\vec{K}) - \langle \mu_{\text{Pd}} \rangle f_{\text{Pd}}(\vec{K}) - P_{11} \mu_{\text{Mn}}^0 F_1(\vec{K}) f_{\text{Mn}}(\vec{K}) \\ & + [-\langle \mu_{\text{Pd}} \rangle + \rho Z_1 + (1-c)^{10} (1-12c) \epsilon \mu_{\text{Mn}}^0] \\ & \times \{1/B(\Gamma)[1 - \Gamma F_1(\vec{K})] - 1\} f_{\text{Pd}}(\vec{K}). \end{aligned} \quad (6)$$

Here, P_{11} is the probability that an atom has eleven Pd nearest neighbors,

$$\Gamma = (1-c) Z_1 J_{\text{PdPd}} \frac{\partial F}{\partial H}, \quad (7)$$

$$\rho \Gamma = (1-c) \frac{\partial F}{\partial \nu}, \quad (8)$$

$$\epsilon = J_{\text{PdMn}} / J_{\text{PdPd}}, \quad (9)$$

$$F_1(K) = \frac{1}{Z_1} \sum_6 e^{i\vec{K} \cdot \vec{\delta}}, \quad (10)$$

and

$$B(\Gamma) = \frac{1}{V} \int_{\text{FBZ}} d^3K \frac{1}{1 - \Gamma F_1(\vec{K})}. \quad (11)$$

Note that the observed $\mathfrak{M}(\vec{K})$ includes positional short-range order while $M(\vec{K})$ refers to the random alloy. These are related by $\mathfrak{M}(\vec{K}) = M(\vec{K})S(\vec{K})$. The $\epsilon \mu_{\text{Mn}}^0$ term actually correlates to the fourth-neighbor shell in this fcc lattice. For simplicity, we take the $K=0$ limit of this term and assume a nearest-neighbor K dependence. This should be a good approximation for these systems because they have large Γ values so the K dependence of the last term in Eq. (6) is determined by $[1 - \Gamma F_1(K)]^{-1}$.

The $M(\vec{K})$ function of Eq. (6) has all the essential features required to reproduce the moment disturbance behavior shown in Fig. 1. The first two terms are all that remain in the spherical average at large K and these are modulated by the last two terms at small K . The third term is a first-neighbor modulation due to the Mn spin reversal. This term becomes more important with increasing Mn content and undoubtedly contributes to the turn down in the small- K region observed for the 0.99- and 1.91-at.% Mn alloys. The last term is the impurity-induced moment disturbance at the Pd sites with a K dependence defined by the magnitude of Γ . If $M(0) = d\bar{\mu}/dc$ for these alloys, the last term must

have a sharp K dependence with correspondingly large Γ values. Unfortunately, we have insufficient small- K data to obtain Γ values for these PdMn alloys. We will therefore extract Γ values from existing PdFe and PdCo data^{7,8} and apply these to the PdMn analysis. This should be valid in the dilute region where Γ approaches that of pure Pd.

With Fe or Co impurities in Pd, there are no antiferromagnetic interactions and no impurity spin reversals. All impurity moments have the same value μ_i and $M(\vec{K})$ becomes

$$\begin{aligned} M(\vec{K}) = & \mu_i f_i(\vec{K}) - \langle \mu_{\text{Pd}} \rangle f_{\text{Pd}}(\vec{K}) + (-\langle \mu_{\text{Pd}} \rangle + \rho Z_1 + \epsilon \mu_i) \\ & \times \{1/B(\Gamma)[1 - \Gamma F_1(\vec{K})] - 1\} f_{\text{Pd}}(\vec{K}). \end{aligned} \quad (12)$$

The observed^{7,8} $M(K)$ functions for 0.26-at.% Fe and 0.3-at.% Co in Pd are shown in Fig. 2. At these concentration levels, $\langle \mu_{\text{Pd}} \rangle \approx 0$ and the last term approaches zero at $K=1$, where $M(1.0) \approx \mu_i f_i(K)$. With $f_{\text{Fe}} = \exp(-0.061K^2)$ and $f_{\text{Co}} = \exp(-0.049K^2)$, $M(1.0)$ yields $3.5\mu_B/\text{Fe}$ and $2.2\mu_B/\text{Co}$ in agreement with the original analysis. $M(K)$ can be fitted to Eq. (12) with the single parameter Γ by assuming $M(0) = d\bar{\mu}/dc$ and evaluating $\rho Z_1 + \epsilon \mu_i$ from the $K=0$ limit of Eq. (12). The resulting Γ values and fitted $M(K)$ functions are shown in Fig. 2. In Ni-Cu and Ni-Rh alloys, Γ approaches

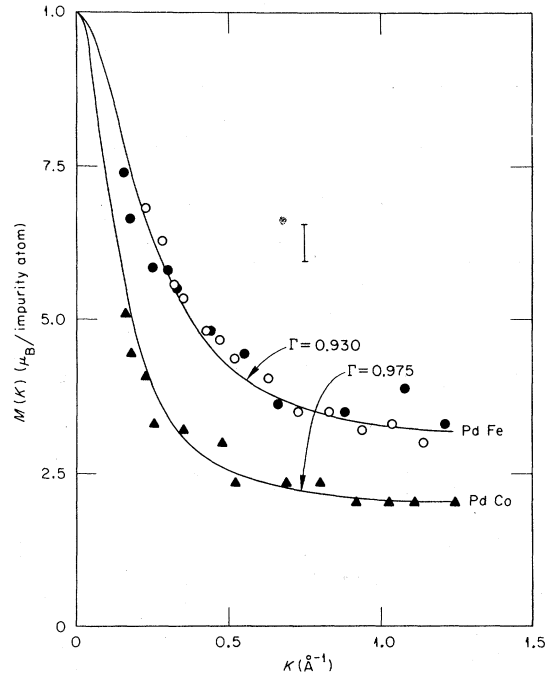


FIG. 2. $\mathfrak{M}(K)$ functions for PdFe and PdCo at the $\frac{1}{4}$ -at.% impurity level. The filled data points are from Ref. 7 and the open points from Ref. 8. The solid curves represent one-parameter fits of the magnetic environment model to the data.

unity at the critical composition for ferromagnetism but decreases to an extrapolated value of $\Gamma_0 = 0.306$ for pure Ni. This shows that the response function $F(H)$ is a saturating function with steeper slopes at lower magnetizations. This saturating effect is much more pronounced in these $PdFe$ and $PdCo$ alloys where the small K increase in $M(K)$ no longer appears above the 3–4-at.% impurity level. Thus the large Γ values obtained here simply indicate that these concentrations are near critical and suggest that the $PdCo$ alloy is closer to the critical composition than the $PdFe$ alloy.

These Γ values obtained for $PdFe$ and $PdCo$ are now used in Eq. (6) to calculate $M(K)$ for the $PdMn$ alloys. For the calculation, $\langle\mu_{Mn}\rangle$ and $\langle\mu_{Pd}\rangle$ are obtained from the large- K data combined with magnetization data by using assumed form factors. The resulting values are given in Table I. μ_{Mn}^0 is obtained from Eq. (5) which yields $\langle\mu_{Mn}\rangle = (1-c)^{12}\mu_{Mn}^0$ while the term $-\langle\mu_{Pd}\rangle + \rho Z_t + (1-c)^{10}(1-12c)\epsilon\mu_{Mn}^0$ is just that required to satisfy $M(0) = d\mu/dc$ in the $K=0$ limit of Eq. (6). Such a calculation gives $M(K)$ for the random alloy whereas some short-range order is to be expected for these alloys. Since $\alpha(R_1) = -0.062$ has been found¹¹ for a 10-at.% Mn alloy, we assume a nearest-neighbor preference for unlike neighbors with $\alpha(R_1)$ proportional to $c(1-c)$ and normalized to the 10-at.% Mn result. The $M(K)$ functions calculated for this degree of short-range order and with $\Gamma = 0.975$ from the $PdCo$ fitting are shown as the solid curves in Fig. 1. These have been forced to satisfy the $M(0) = d\mu/dc$ relation, but also reproduce the observed $M(K)$ behavior reasonably well. Better agreement could be obtained by assuming a longer-ranged ($\sim 5 \text{ \AA}$) Mn spin-reversal correlation, but this refinement would not change the general conclusions nor the individual moment values obtained.

CONCLUSIONS

The polarized-neutron $\mathfrak{M}(K)$ functions and the bulk magnetization data for $PdMn$ alloys can be brought into agreement by assuming a long-ranged impurity-induced moment disturbance in the Pd similar to that found^{7,8} for $PdFe$ and $PdCo$ alloys. A one parameter magnetic environment model is shown to reproduce this moment disturbance in $PdFe$ and $PdCo$ with parameters in the expected range. The same parameters carried over to the $PdMn$ case are consistent with the observations which are, however, severely limited in the small- K region where most of this effect occurs. At the 1- to 2-at.% Mn level the $\mathfrak{M}(K)$ functions show evidence of an anticorrelation which we interpret as the combined effects of positional short-range

TABLE I. Individual magnetic moments of $PdMn$ alloys at 4.2 K and 45 kOe.

at.% Mn	$\bar{\mu}^a$	$\langle\mu_{Pd}\rangle$	$\langle\mu_{Mn}\rangle$	μ_{Mn}^0 ^b
0.23	0.016	0.008	3.6	3.7
0.46	0.030	0.012	4.0	4.3
0.99	0.058	0.024	3.5	4.0
1.91	0.099	0.034	3.5	4.4
	$\pm 1\%$	$\pm 10\%$	± 0.3	± 0.3

^a Bulk magnetizations from Ref. 2 expressed in μ_B/atom .

^b From $\langle\mu_{Mn}\rangle = (1-c)^{12}\mu_{Mn}^0$.

order and Mn spin reversal. The configurational aspects of the Mn spin reversal and the response of antiparallel Mn atom pairs to an applied field is crucial to understanding the magnetization behavior of these alloys. In the model we have used, only the fraction $(1-c)^{12}$ of the Mn atoms have all Pd nearest neighbors and, with their surrounding Pd polarization clouds, are free to respond to an applied field. The remaining Mn moments in these dilute alloys are coupled together in antiferromagnetic pairs and this coupling must be broken down by the applied field before magnetization can occur. Star, Foner, and McNiff² find normal Brillouin behavior at very low Mn content where there are essentially no Mn atom pairs, but departures from this at higher Mn levels where the field required for saturation increases with increasing Mn content. They estimate that an antiferromagnetic coupling as large as 50 K is required to describe their high-field magnetizations within the molecular field model. In that case, the 45 kOe applied in this experiment produces essentially no magnetization of the Mn atom pairs ($\mu H/kT \approx 0.24$ for $\mu_{Mn}^0 = 4\mu_B$), but about 96% saturation of the isolated Mn moments and their associated polarization clouds. The $\langle\mu_{Pd}\rangle$ and $\langle\mu_{Mn}\rangle$ values in Table I should therefore be increased by about 4% to obtain the saturation values. The μ_{Mn}^0 values are obtained from $\langle\mu_{Mn}\rangle = (1-c)^{12}\mu_{Mn}^0$ and thus correspond to the random alloy with a nearest neighbor spin reversal mechanism. Actually, the short-range order in these alloys tends to isolate the Mn atoms and this would decrease μ_{Mn}^0 . On the other hand, a longer-ranged spin-reversal mechanism would tend to increase μ_{Mn}^0 . Because of these uncertainties, the best μ_{Mn}^0 determination comes from the two more dilute alloys for which we obtain $(3.8 \pm 0.3)\mu_B$ and $(4.4 \pm 0.3)\mu_B$ at saturation. These are significantly smaller than was deduced from the specific-heat⁹ and unpolarized neutron¹⁰ data but are consistent with the expected electronic configuration of a Mn atom dissolved in Pd.

ACKNOWLEDGMENTS

The authors are indebted to D. E. LaValle for sample preparation, to D. K. Christen and R. H.

Kernohan for the magnetization measurements, and to J. L. Sellers for assistance in the neutron measurements.

*Research sponsored by the ERDA under contract with Union Carbide Corp.

†Present address: IVIC, Apartado 1827, Caracas, Venezuela.

¹W. M. Star, S. Foner, and E. J. McNiff, *Phys. Lett. A* **39**, 189 (1972).

²W. M. Star, S. Foner, and E. J. McNiff, *Phys. Rev. B* **12**, 2690 (1975).

³J. Crangle, *Philos. Mag.* **5**, 335 (1960).

⁴R. M. Bozorth, P. A. Wolff, D. D. Davis, V. B. Compton, and J. H. Wernick, *Phys. Rev.* **122**, 1157 (1961).

⁵J. W. Cable, E. O. Wollan, and W. C. Koehler, *J. Appl. Phys.* **34**, 1189 (1963).

⁶J. W. Cable, E. O. Wollan, and W. C. Koehler, *Phys. Rev. A* **138**, 755 (1965).

⁷G. G. Low and T. M. Holden, *Proc. Phys. Soc. Lond.* **89**, 119 (1966).

⁸T. J. Hicks, T. M. Holden, and G. G. Low, *J. Phys. C* **1**, 528 (1968).

⁹B. M. Boerstoel, J. J. Zwart, and J. Hansen, *Physica (Utr.)* **57**, 397 (1972).

¹⁰C. J. de Pater, C. van Dijk, and G. J. Nieuwenhuys, *J. Phys. F* **5**, L58 (1975).

¹¹N. Ahmed and T. J. Hicks, *J. Phys. F* **4**, L124 (1974).

¹²J. W. Cable, E. O. Wollan, W. C. Koehler, and H. R. Child, *Phys. Rev.* **128**, 2118 (1962).

¹³A. M. Clogston, *Phys. Rev. Lett.* **19**, 583 (1967).

¹⁴R. A. Medina and J. W. Cable, *Phys. Rev. B* **15**, 1539 (1977).

¹⁵J. W. Cable, *Phys. Rev. B* **15**, 3477 (1977).